Frequency Trimming and *Q*-Factor Enhancement of Micromechanical Resonators Via Localized Filament Annealing

Kun Wang, Ark-Chew Wong, Wan-Thai Hsu, and Clark T.-C. Nguyen

Center for Integrated Sensors and Circuits
Department of Electrical Engineering and Computer Science, 2406 EECS Bldg.
University of Michigan
Ann Arbor, Michigan 48109-2122 USA
email: ctnguyen@eecs.umich.edu

SUMMARY

A batch-compatible, post-fabrication annealing technique based upon filament-like heating of microstructures is demon-strated as an effective means for trimming the resonance fre-quencies (f_o's) and increasing the quality factors (Q's) of surface-micromachined, polysilicon, mechanical resonators. Although the technique is straightforward, involving the mere application of a suitable voltage between the anchors of a micromechanical resonator, it provides a substantial range of adjustment, with frequency trims of over 2.7% and Q increases of up to 600%, depending upon resonator fabrication history. By pulsing the anneal voltage waveforms, controlled frequency trims of less than 16 ppm per trial are achievable.

Keywords: trim, resonator, anneal

I. INTRODUCTION

With the advent of frequency specific applications for micromechanical resonators, such as oscillator references [1] and highly selective bandpass filters [2,3], techniques for post-fabrication trimming of resonance frequencies are becoming increasingly important. This is especially true for recent com-munications applications of micromechanical resonators, in which large numbers of such resonators with precisely located center frequencies must realize parallel filter banks and multiple oscillator references [1]. Since these applications will likely be batch-fabricated using planar technologies, high throughput trimming is desirable.

This paper describes a novel procedure for both trimming the frequency and altering the quality factor of micromechani-cal resonators. The technique, from this point on referred to as "localized" or "filament" annealing, involves sending a current through a micromechanical structure, thus dissipating power in the structure and achieving temperatures high enough to anneal it. This annealing alters both the structure's resonance fre-quency and its quality factor, and can be implemented in a very simple fashion, making it amenable to batch trimming of micro-mechanical devices. In combination with intelligent control cir-cuitry, such a batch trimming capability could greatly impact the manufacture of resonator-based gyros [4] and precision fre-quency references [1], and can possibly serve as an enabling technology for devices requiring large numbers of matched, high-Q μmechanical resonators, such as high-order microme-chanical communications filters [1,2].

II. THE BASIC ANNEALING TECHNIQUE

Figure 1 presents a schematic depicting details of this fila-ment annealing procedure as applied to a properly biased and excited comb-driven, folded-beam μmechanical resonator [5] with sense electronics. The resonator design is similar to prede-
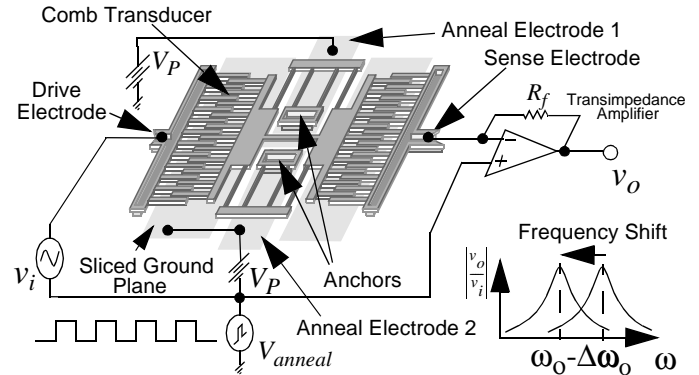

Fig. 1: Perspective-view schematic depicting details of the filament annealing procedure, showing circuit details and indicating key components.

cessors [5] in all respects, except for the provision of distinct leads to both anchor points. During normal resonator operation, the pulse voltage generator v_{anneal} is inactive and provides the ground voltage for all components in this resonator system. In this configuration, the anchor leads along with the ground plane are tied to the dc-bias voltage V_P, and an ac signal is applied to one or more of the transducer electrodes to induce vibration. Once vibration is established, an output current is generated via the dc-biased, time-varying capacitor at the output electrode. This current is then sensed and amplified to a voltage by the transresistance amplifier.

To anneal the μresonator, the pulse voltage generator v_{anneal} is activated. Depending on the requirements, v_{anneal} is made to emit one or more voltage pulses of magnitude V_{anneal} for each annealing cycle. During each pulse, the potentials of the input and output electrodes, the ground plane, and one of the resonator anchors are raised by V_{anneal}, while the potential at the remaining resonator anchor remains constant at V_P. Thus, each pulse effectively applies a voltage across the resonator, from anchor to anchor, of magnitude V_{anneal}, which then sources a current I_{anneal} from anchor to anchor. This current flows through the resonator structure, dissipating a power given by

$$P_{anneal} = I_{anneal}^2 R_{struct}, \qquad (1)$$

where R_{struct} is the resistance between the anchors of the reso-nator. Heat is thus generated throughout the resonator structure, raising its overall temperature and effectively annealing it.

Due to variations in electrical and thermal resistance along the resonator length between anchor points, different locations along the resonator structure attain different temperatures dur-ing any given annealing cycle. For a given value of V_{anneal}, the temperature at a specific location can be found using a distrib-

Table I: Micromechanical Resonator Data

Parameter	Value	Units
Folded-Beam Length, L	25	μm
Folded-Beam Width, W	2	μm
Structural Layer Thickness, h	2	μm
Effective Mass, m	3.19×10^{-11}	kg
System Spring Constant, k	309.74	N/m
No. Finger Overlaps at Port 1, N_{g1}	52	—
No. Finger Overlaps at Port 2, N_{g2}	52	—
Finger Gap Spacing, d	1	μm
Finger Overlap, L_d	5	μm
$\partial C / \partial x$ per Finger Overlap	1.25×10^{-12}	F/m
Nominal Resonance Frequency, f_o	455	kHz
Top Surface Area of Shuttle, $A_{shuttle}$	9000	μm^2
Anchor-to-Anchor Resistance, R_{struct}	1400	Ω
Resistivity, ρ	0.01	Ω cm

Hottest points
T=1311°C
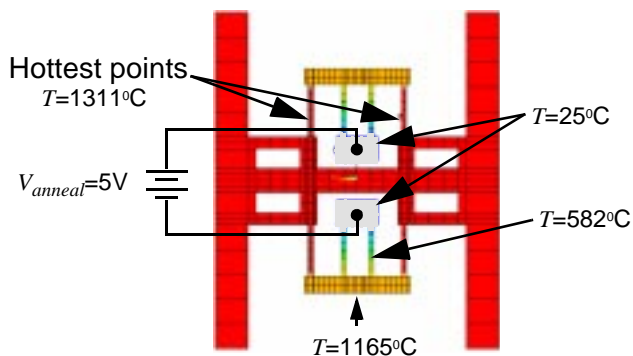T=25°C
V_{anneal}=5V
T=582°C
T=1165°C

Fig. 2: Temperature profile on the micromechanical resonator for a constant applied V_{anneal} as determined using ANSYS.

uted approach, where the resonator structure is first sectioned into numerous power elements, and temperature contributions from each element are then superposed at the desired location. A program was written to implement this procedure using equivalent thermal circuits to model resonator thermal behavior. Applying this program to the resonator of this work (summarized in Table I), the hottest location during an annealing cycle is found to be at the outer suspension beams, near the shuttle. This analytical result is verified by both finite-element analysis (Fig. 2) and experiment (Fig. 3). For a constant V_{anneal}=5V, the temperature T_x at this hottest location (assuming no convection) is 1311°C; for V_{anneal}=7V, T_x=1500°C; and for V_{anneal}=8V, T_x=1750°C. For V_{anneal}=8V, the pulse duration must be shorter than 3 ms to avoid destroying the device.

For the case of pulsed voltage annealing, the temperature at a given location will also be a function of pulse duration and spacing, especially if the duration is much less than the thermal time constant of the resonator structure. Using an equivalent thermal circuit model for the resonator, the thermal time constant for the resonator summarized in Table I is calculated to be τ_{th}=2.4 ms, which means a step function of v_{anneal} with a magnitude of 7V can heat the suspending beams up to ~900°C in just 2 ms. Thus, the described filament annealing technique is equivalent to an exceptionally fast rapid thermal annealing
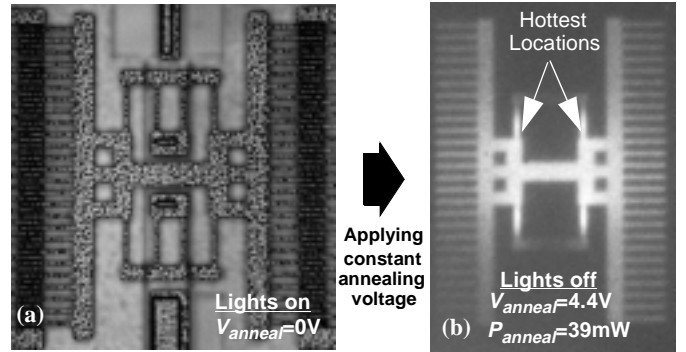

Fig. 3: Overhead photographs of a micromechanical resonator (a) at room temperature; and (b) under a constant applied V_{anneal} voltage, clearly indicating the hottest locations as the brightest spots.

Table II: Doping Recipes

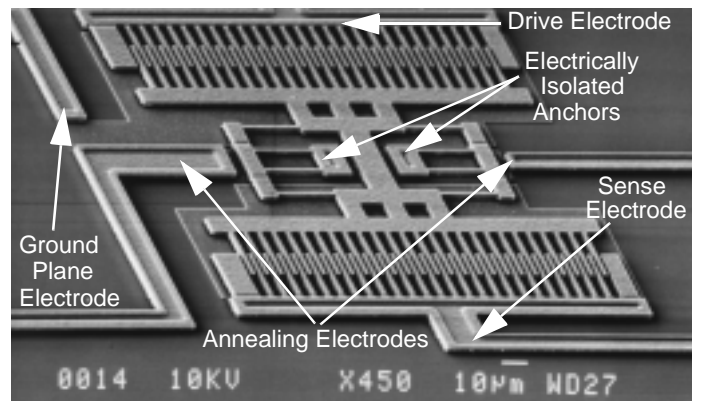| POCl$_3$	Implant
(i) Deposit 2 μm LPCVD fine-grained polysilicon @ 588°C	(i) Deposit 1 μm LPCVD fine-grained polysilicon @ 588°C
(ii) Dope 2.5 hrs. @ 950°C in POCl$_3$ gas	(ii) Implant phosphorous: Dose=10^{16} cm^{-2}, Energy=90 keV
(iii) Anneal for 1 hr. @ 1100°C in N$_2$ ambient	(iii) Deposit 1 μm LPCVD fine-grained polysilicon @ 588°C
	(iv) Anneal for 1 hr. @ 1100°C in N$_2$ ambient

Fig. 4: SEM of a fabricated folded-beam resonator, equipped with leads for filament annealing.

(RTA) process. In addition, by choosing pulses with durations from 1-5 ms, and spacing them by designed amounts, a wide variety of annealing cycles can be implemented [6].

III. EXPERIMENTAL RESULTS

Folded-beam resonators with accommodations for filament annealing were designed to the specifications of Table 1 and fabricated via two variants of a standard polysilicon surface-micromachining technology: one in which the structural material was doped via POCl$_3$ at 950°C in a furnace; and another in which the structural material was implanted. Recipes for each doping process are summarized in Table II. Figure 4 presents the scanning-electron micrograph (SEM) of a completed resonator, identifying key components used for filament annealing.
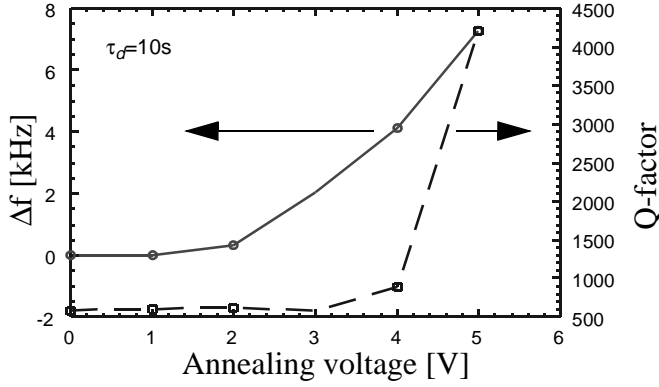
Fig. 5: Measured frequency spectra after filament annealing for 10 seconds at various voltages, showing both frequency adjustment and Q-enhancement.
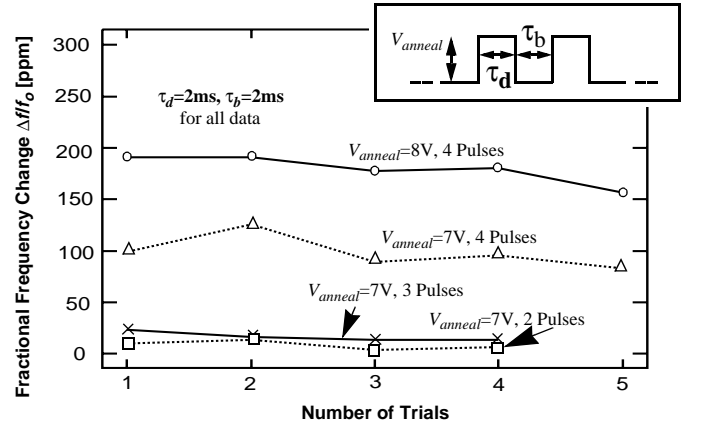

Fig. 6: Plot of frequency change versus anneal trial with the number of pulses as a third variable, indicating some consistency from trial to trial for a given resonator.
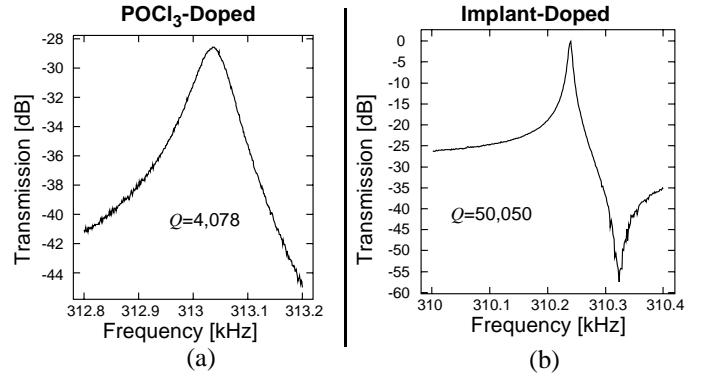

Fig. 7: Measured transconductance spectra for a $POCl_3$-doped resonator (a) and an implant-doped version (b), both before filament annealing and plotted over the same range.

Following fabrication and release, wafers were diced, packaged, and bonded into metal DIP packages, with careful attention to grounding for suppression of parasitic feedthrough. These packages were then interfaced with electronics at the circuit board-level, then inserted into a custom-built vacuum test chamber that featured low capacitance feedthroughs for interfacing with external instrumentation. A turbomolecular pump was then used with this chamber to achieve operating pressures down to 40 microTorr, where Q-degradation due to gas damping is negligible.

The above apparatus was utilized in combination with an HP4195A Network/Spectrum Analyzer to measure transconductance spectra for annealed resonators, from which resonance frequency f_o and Q were then extracted. All measurements were performed under 40 microTorr vacuum using V_P=100V and v_i=10mV, for which vibration amplitudes remained well within the linear region of operation (i.e., no Duffing present) [9].

Frequency Trimming Data.

Using these resonators, experiments were conducted in which structures where systematically annealed using sequences of specific (V_{anneal}, τ_d, τ_b) sets, where τ_d is pulse duration, and τ_b is the spacing between pulses (for multiple pulse anneals). After each anneal, the frequency spectrum of the resonator-under-test was measured to determine f_o and Q. The data from several such experiments are summarized in Figs. 5 and 6.

Figure 5 plots frequency change Δf and Q versus V_{anneal} for the case of long (τ_d=10s) anneals, and dramatically illustrates the degree of change possible in the frequency (f_o) and Q of a polysilicon, implant-doped resonator when post-fabrication filament annealing is applied. From the data, low values of V_{anneal} are seen to be ineffective, which implies an activation energy-dependence. Over the duration of the experiment, the Q of this particular resonator increased from 580 to 4200—an improvement of more than 600%. This was the largest percentage increase observed in these experiments.

Although long anneals can induce significant, permanent frequency shifts in released micromechanical resonators, they are not conducive to precise trimming of frequencies. For better precision, short pulses on the order of milliseconds are more appropriate. Figure 6 presents a plot of fractional frequency change versus trial with the number of pulses per trial as a third variable. For each trial, V_{anneal}=7V, τ_d=2 ms, and τ_b=4 ms (i.e., a 50% duty cycle was used). As shown, although little or no fre-

quency change was seen for one and two pulse anneals, the frequency change per trial was very consistent for three and four pulse anneals. In addition, $\Delta f/f_o$ increased with the number pulses for these cases, which suggests some influence from total annealing time and/or thermal cycling [6] on the frequency change per trial.

It should be mentioned that for this work, over 98% of the resonators tested exhibited a decrease in frequency after sufficient filament annealing. A very small portion of the devices actually went up in frequency by large amounts (with large, correlated Q changes) after the first anneal cycle, but then consistently went downward in frequency for anneal cycles immediately afterwards. This is indicative of a dramatic change in material parameters, most likely stress, after the first anneal cycle, then a settling down into predictable behavior afterwards. The observed change in the direction of frequency shift also agrees with previously reported data in which RTA annealing changed the stress profile in polysilicon thin films from compressive to tensile [7].

Q-Enhancement.

Figure 7 presents measured transconductance spectra for a $POCl_3$-doped resonator and an implant-doped version, both before filament annealing. The implant-doped resonator exhibits an order of magnitude higher Q than its $POCl_3$-doped counterpart, suggesting a very strong dependence of resonator quality on doping technique. Given that $POCl_3$-doping inflicts surface and internal damage to silicon materials, often generating large concentrations of edge and point dislocations within

Table III: Annealing Effectiveness vs. Doping Method

Parameter	Doping Method			
	POCL3 #1	POCL3 #2	I/I #1	I/I #2
f_{before} [Hz]	320,350	241,702	313,781	280,777
Q_{before}	166	515	19,000	40,120
f_{after} [Hz]	309,587	233,899	305,429	280,770
Q_{after}	429	1,024	43,000	41,350
Δf [Hz]	10,763	7,803	8,352	7
ΔQ	263	509	24,000	1,230

the material, the above result suggests that the dominant loss mechanism that limits Q in POCl$_3$-doped resonators is related to the defect density in the structural material. This is consistent with previous findings for macroscopic quartz and sapphire resonators [8].

It should be mentioned that the higher concentration of phosphorous in POCl$_3$-doped polysilicon versus implant-doped polysilicon resonators is not a likely reason for its substantially lower Q. This follows from previous observations that the Q of *in situ* phosphorous-doped polysilicon folded-beam µresonators can be on the order of 80,000 under microTorr pressures [9], despite degenerate phosphorous doping.

By application of filament annealing to these structures, further insight into Q-limiting loss mechanisms is obtained. Table III presents the f_o's and Q's versus successive filament anneals for several POCl$_3$- and implant-doped resonators. Several important observations are worth mentioning:

(1) It is evident that implant-doped resonators not only start out with higher Q, they are also more conducive to Q-enhancement via filament annealing, showing more than 100% increase in Q for some resonators. On the other hand, although filament annealing does increase the Q of POCl$_3$-doped resonators, it is unable to raise it substantially.

(2) Large shifts in Q are always accompanied by correspondingly large shifts in f_o, and likewise for small shifts. This suggests some degree of correlation.

(3) There is some maximum Q limit attainable using filament annealing. When this limit is reached, frequency is no longer trimmable over large ranges.

The above observations suggest that under high vacuum conditions, the energy dissipation per cycle (related to Q) in implant-doped resonators is dominated by stress-relaxation mechanisms [8]. Rapid thermal annealing via this filament technique then provides a method by which stress and its associated high energy state can be greatly alleviated, resulting in simultaneous shifts in the f_o and Q of the resonator. One might tentatively postulate that doping by implantation creates stress-derived defects that are not removed completely via furnace annealing, but that can be annealed away through post-fabrication, high-speed, filament annealing. Although this is consistent with mechanisms proposed in [8], it is still stated tentatively, pending further study.

For the case of POCl$_3$-doped resonators, however, filament annealing has a much smaller effect on the Q, although frequency trimming is still possible at ppm levels. This is not unexpected if one assumes that the majority of Q-limiting dislo-

cations generated via POCl$_3$-doping are independent of stress, and thus, unaffected by filament annealing. As a consequence, the maximum Q attainable via filament annealing of POCl$_3$-doped resonators is much smaller than that of their implant-doped counterparts.

IV. CONCLUSIONS

A convenient post-fabrication annealing technique based upon filament-like heating of microstructures has been shown to both trim the frequencies and enhance the Q of polysilicon micromechanical resonators. The degree of trim and Q control is a strong function of the method used to dope the structures, and most probably, of many other process-related variations. Nevertheless, the frequency shifts per resonator have shown a degree of consistency that makes filament annealing attractive as the basis for a batch trim technique, provided a fabrication process that yields repeatable stress profiles is utilized.

Experiments using this filament annealing technique have also provided insight into loss mechanisms that limit resonator Q. In particular, the Q's of implant-doped polysilicon resonators can be greatly enhanced via filament annealing, whereas the Q's of POCl$_3$-doped polysilicon resonators with substantial surface roughness were found to be much less affected. Annealing data suggests some correlation between stress, frequency, and Q.

REFERENCES

[1] C. T.-C. Nguyen, "Micromechanical resonators for oscillators and filters," *Proceedings*, 1995 IEEE International Ultrasonics Symposium, Seattle, WA, Nov. 7-10, 1995, pp. 489-499.

[2] Kun Wang and C. T.-C. Nguyen, "High-order micromechanical electronic filters," *Proceedings*, 1997 IEEE International Micro Electro Mechanical Systems Workshop, Nagoya, Japan, Jan. 26-30, 1997, pp. 25-30.

[3] F. D. Bannon III, J. R. Clark, and C. T.-C. Nguyen, "High frequency microelectromechanical IF filters," *Technical Digest*, IEEE International Electron Devices Meeting, San Francisco, California, December 8-11, 1996, pp. 773-776.

[4] M. W. Putty and K. Najafi, "A micromachined vibrating ring gyroscope," *Technical Digest*, Solid-State Sensor and Actuator Workshop, Hilton Head Island, S. C., June 13-16, 1994, pp. 213-220.

[5] W. C. Tang, T.-C. H. Nguyen, and R. T. Howe, "Laterally driven polysilicon resonant microstructures," *Sensors and Actuators,* **20**, 25-32, 1989.

[6] K. Wang, D. Pavlidis and J. Cao, "Effect of In Situ Thermal Cycle Annealing on GaN Film Properties Grown on (001) and (111) GaAs, and Sapphire Substrates," *J. of Elec. Mat.*, vol. 26, No. 1, 1997

[7] X. Zhang, T.-Y. Zhang, M. Wong, and Y. Zohar, "Effects of high-temperature rapid thermal annealing on the residual stress of LPCVD-polysilicon thin films," *Proceedings*, IEEE International Micro Electro Mechanical Systems Workshop, Nagoya, Japan, Jan. 26-30, 1997, pp. 535-540.

[8] V. B. Braginsky, V. P. Mitrofanov, and V. I. Panov, *Systems With Small Dissipation.* Chicago: University of Chicago Press., 1985.

[9] C. T.-C. Nguyen and R. T. Howe, "CMOS Micromechanical Resonator Oscillator," *Technical Digest,* IEEE International Electron Devices Meeting, Washington, D. C., pp. 199-202, December 5-8, 1993.